JOURNAL OF SPACECRAFT AND ROCKETS
Vol. 41, No. 6, November–December 2004

Anomalous Force on the Wilkinson Microwave Anisotropy Probe

Scott R. Starin,* James R. O'Donnell Jr.,† David K. Ward,‡ and Edward J. Wollack§
NASA Goddard Space Flight Center, Greenbelt, Maryland 20771
P. Michael Bay¶
Jackson and Tull, Lanham-Seabrook, Maryland 20706
and
Dale R. Fink**
Computer Sciences Corporation, Lanham-Seabrook, Maryland 20706

The Wilkinson Microwave Anisotropy Probe orbits the outer Earth–sun libration point, about 1.5 million kilometers outside Earth's orbit, mapping cosmic microwave background radiation. To achieve its orbit on a small fuel budget, the spacecraft needed to perform a lunar gravity assist maneuver. Timing the lunar swing-by required the spacecraft to travel in three high-eccentricity phasing loops with critical maneuvers at a minimum of two, but nominally all three, of the perigee passes. On the approach to the first perigee maneuver, spacecraft telemetry showed a considerable change in system angular momentum that threatened to cause the onboard failure detection and correction software to abort the critical maneuver. Fortunately, the system momentum did not reach the preset failure detection limit; however, the mission operations team did develop a contingency strategy should a stronger anomaly occur before or during subsequent perigee maneuvers. Simultaneously, the team developed and tested various hypotheses for the cause of the anomalous force. The final hypothesis was that water was outgassing from the thermal blanketing and freezing to the cold side of the solar shield. As radiation from Earth warmed the cold side of the spacecraft, the uneven sublimation of ice created a torque on the spacecraft.

Nomenclature

$H_{\max}$	=	peak angular momentum, Nm · s
k_b	=	Boltzmann constant, 1.38×10^{-23} J/K
L_2	=	outer Earth–sun libration point
m_o	=	total initial outgassing mass, kg
N	=	atomic mass, amu
n	=	heating event index
P_{final}	=	third and final perigee
P_1	=	first perigee of the mission
P_2	=	second perigee
R	=	average moment arm from center of mass, m
T	=	estimated temperature of sublimating material, K
t	=	elapsed mission time, days
u	=	atomic mass unit, 1.66×10^{-17} kg
V_{kin}	=	average velocity of sublimating material, m/s
Δm	=	ejected mass, kg
τ	=	outgassing time constant, days

Introduction

THIS paper describes an anomalous force that acted on the Wilkinson Microwave Anisotropy Probe (WMAP) in a puzzling way. For background information, please refer to Bennett et al.[1] for WMAP science and Markley et al.[2] for WMAP engineering. The force acted each time WMAP approached perigee in preparation for its crucial orbit-raising maneuvers, and it reappeared at the periselene, the lunar swing-by to which those maneuvers directed the spacecraft.

Received 10 December 2002; revision received 6 November 2003; accepted for publication 18 November 2003.

*Aerospace Engineer. Member AIAA.
†Senior Aerospace Engineer. Senior Member AIAA.
‡GNC Lead Engineer. Senior Member AIAA.
§Astrophysicist.
¶Mission Systems Engineer. Member AIAA.
**Senior Computer Scientist.

Though in hindsight the presence of this anomalous force would not have ended the mission, the potential threat presented by such a mysterious and possibly unpredictable event was considerable at the time. Combined with the criticality of the mission operations occurring at its first appearance, the anomaly engendered one of the most challenging operations that faced the WMAP team during the in-orbit checkout and maneuvering phase of the mission.

WMAP Spacecraft

Configuration

The WMAP Observatory is composed of three main portions: the instrument, the central truss, and the solar shield. Figure 1 shows the upright spacecraft, with the instrument, its optics, and its large thermal radiators on top of the hexagonal central truss. The passively cooled portions of the instrument operate at a physical temperature of about 60–100 K. Providing a cold and extremely stable thermal environment is vital to achieving the mission's science objectives.

To the central truss is attached the rest of the vital spacecraft components. At the bottom of Fig. 1, and shown also in Fig. 2, is the solar shield, which comprises the six solar array panels, thermal blankets stretched between those panels, and several components (e.g., sun sensors) that need to be exposed to the sun.

A key thermal design feature is that the backside of the solar shield is insulated from the sun-facing side, improving the passive cooling of the instrument required for science observations. Also of particular interest in this paper, the coarse sun sensors (CSS) are located in redundant pairs at the outer ends of the array panels. The CSSs on panels 1, 3, and 5 face toward the sun at a 57-deg cant from the *XY* plane, and the CSSs on panels 2, 4, and 6 face away from the sun with the same cant; the cold-side CSSs nominally receive no signal during science operations. Figure 2 shows the identifying numbers in relation to the spacecraft axes. Figure 3 shows the trajectory followed by WMAP as it was guided toward L_2.

Nominal Perigee Maneuver Plan

Before each maneuver, WMAP was in its science observation mode, and the first command to prepare for a maneuver was to exit this mode. The spacecraft was then put into its inertial pointing mode for the preburn period. This mode established the desired attitude, which would be aligned with the correct direction of velocity change at the burn start, in advance via commanded quaternion.

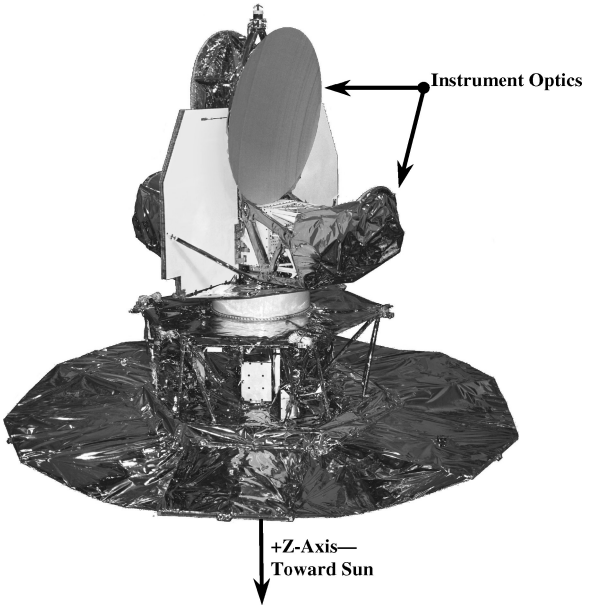

Fig. 1 WMAP observatory: solar shield deployed.

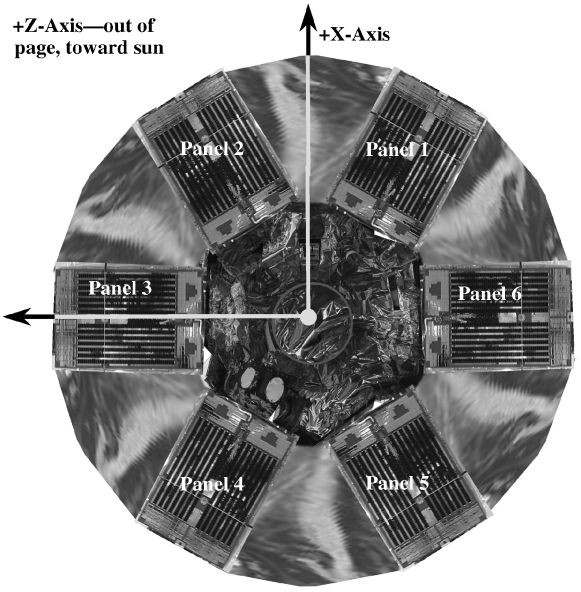

Fig. 2 Sun side of deployed WMAP solar shield showing solar-array panel numbering.

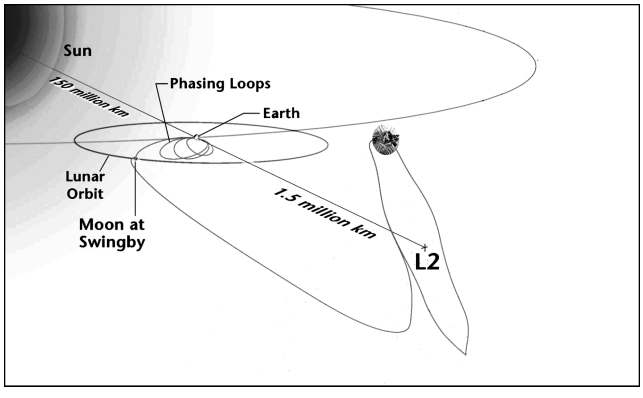

Fig. 3 Early operations trajectory plan.

Each perigee pass used a slightly different attitude, but in all cases the spacecraft and its arrays were oriented about 45–50 deg from the sun, and the instrument was directed approximately toward nadir at perigee. These factors combined to create an attitude profile that allowed the sun to heat the instrument and Earth albedo to illuminate the cold side of the solar shield shortly before perigee. These were the only times after launch that these cold surfaces were illuminated.

At the burn start, the spacecraft was commanded into the thruster control mode for changing orbital velocity (Delta V), which also used commanded quaternions to follow the correct trajectory. Next, the Delta V mode autonomously exited into the thruster control mode for changing angular momentum (Delta H) at the completion of the burn. Finally, after the Delta H mode dumped momentum a stored command put the spacecraft into its sun acquisition mode.

Anomaly at First Perigee

About 40 min before P_1, WMAP telemetry showed a small but significant increase in system angular momentum. The momentum continued to grow for approximately 17 min, with the total (i.e., root-sum-squared) system momentum increasing from 0.5 to 1.6 Nm · s (Fig. 4). To protect against a thruster malfunction during a maneuver, onboard failure detection and correction (FDC) was configured to abort a burn at 5 Nm · s of system momentum. At the observed rate of growth, it seemed the limit could have been reached, and FDC would have aborted the maneuver just before it started. After a few tense minutes, it became clear that the system momentum rate of growth was slowing for the moment. There was still some concern, however, that the increased momentum could cause an unacceptable transient when the maneuver started.

The system momentum peaked 20 min before perigee; it then decreased significantly, but not to its preanomaly level, over the next 15 min. Operations in Delta V mode started about 5 min before perigee, as scheduled, and concluded without incident. Because the Delta V mode also acts to reduce system momentum, it was difficult to obtain information regarding the momentum change after the thrusters began to fire. However, after Delta H mode left the spacecraft at a safe system momentum of about 0.4 Nm · s, the system momentum decreased as a result of continuing external torque disturbances by an additional 0.1 Nm · s before settling to a constant value.

Analysis of Anomalous Force

In each case, a negative change in Y-axis momentum was observed first, suggesting a nose-up moment (note that this is opposite of aircraft convention because the WMAP $+Z$ axis pointed upward). This negative Y-axis torque was associated with an increase in the system momentum magnitude. The nose-up momentum increase was followed by both a negative roll moment ($-X$ torque) and a nose-down moment ($+Y$ torque). The Y-axis momentum returned nearly to its original value just before the burn, and the X-axis momentum had a small offset.

While a modified operations plan to guarantee good maneuver performance was being developed, the WMAP team was also active in attempting to diagnose the problem to predict the future behavior of the force. The culmination of this effort was a model that accurately predicted the magnitudes of the system momentum changes seen at P_{final} and periselene. The reasoning used in the elimination of more mundane causes and the development of the accepted theory follow.

Sensor or Actuator Malfunction

During the anomaly, a quick look at other telemetry points suggested that the anomaly was the result of a true torque rather than a sensor or actuator malfunction. It was known that there was some error in the reaction wheel tachometer scaling factors by that time, but such errors would have affected momentum telemetry only if the attitude had been changing, causing the stored momentum to be traded between the wheels. However, the inertial reference units and digital sun sensors corroborated that the attitude was not changing. The reaction wheels were behaving properly by absorbing the change in system momentum and maintaining the desired attitude profile.

It was postulated that the spinning reaction wheels might have been tipped by thermal deflection of the deck. This hypothesis was not credible, though, because the wheels were spinning too slowly to act as control moment gyros. Another idea was that, because of a problem with the reaction wheel electronics, false speeds could have been indicated, thus creating a virtual source of momentum. It was extremely unlikely, however, that the signature seen could have had this cause. The wheel axes were aligned such that only a very particular and complex combination of failures in all three wheels could have resulted in false X- and Y-axis momentum readings with very small Z-axis changes.

Typical Disturbance Torque Sources

Shortly after P_1, team members began to offer hypotheses for the anomalous force. The first hypothesis was gravity-gradient torque because the torque occurred close to Earth and the time-varying momentum profile could correspond to the movement of the nadir vector with respect to the spacecraft body axes. The maximum gravity-gradient torque was calculated assuming a 45-deg angle with nadir and using the known mass properties of the Observatory. Three other near-Earth disturbance torques—atmospheric drag, solar radiation pressure, and magnetic field—were calculated at that time. (See Larson and Wertz[3] for equations to calculate typical disturbance torques.) Table 1 shows the maximum magnitude for each of the disturbance torques. The atmospheric calculation uses an average value for atmospheric density, and it assumes a moment arm of 3 m, which approximates the height of the entire Observatory. The same moment arm was used for the solar pressure torque, along with a maximal reflectivity of unity. Finally, the magnetic torque figure uses the predicted maximum residual dipole for WMAP of 0.8 amp-turn-m^2.

This simple, worst-case magnitude analysis was sufficient to eliminate all four possibilities. The solar radiation torque had the greatest maximum magnitude of the four; despite the estimation of a very large moment arm for the torque, the magnitude was still a factor of six less than the observed maximum torque of 0.004 Nm at P_1. In addition, the solar radiation pressure could not have caused a time-varying torque because the attitude with respect to the sun was held strictly constant until the thrusters began to fire. Analysts were forced to turn to more exotic hypotheses to explain the phenomenon.

Table 1 Maximum magnitudes of common disturbance torques

Disturbance torque	Value, Nm
Gravity gradient	6.0×10^{-5}
Atmospheric drag	1.2×10^{-8}
Solar radiation pressure	6.8×10^{-4}
Magnetic field	1.6×10^{-5}
Actual disturbance	4.0×10^{-3}

Propellant Leak

The possibility of thruster leakage was considered. If any one thruster had been leaking, the resulting change in momentum would have been in one of the eight particular, known thruster torque directions, and would have resulted in a specific combination of X-, Y- and Z-axis changes to momentum. Though the first few minutes of the anomaly allowed the possibility of a leak in thruster 4, which only provides negative pitching moment, the later changes in X-axis momentum discounted that hypothesis.

Thermal Bending

Differential heating of the solar-array panels and their attached blankets could have bent these components, resulting in a compensating rotation of the spacecraft hub. This explanation was the first that seemed consistent with the time profile of the torques. However, calculations ruled out this possibility as well; any momentum imparted to the spacecraft body by warping solar arrays and blankets would have required equal and opposite momentum in the arrays and blankets. The 2-Nm · s peak momentum observed implied a sustained angular rate, about 1–3 deg/s for several seconds, based on the moments of inertia of the arrays and the blankets, that would have exceeded any motion which could have actually occurred in the arrays. These rates indicated that the array tips would have been deflected ~0.05 m/s for several minutes. On WMAP, such movement would have resulted in the arrays closing entirely, which certainly did not occur.

Illumination of Antisun Side of Solar Shield

Figures 5 and 6 show CSS profiles scaled and superimposed over the X- and Y-axis momentum profiles for P_1 and P_2. The torques appeared to occur as the three dark-side CSSs were illuminated by Earth albedo during the perigee approaches. Furthermore, the order of illumination (first CSS 2, then 6, then 4) indicated a correspondence between albedo varying across the cold side of the solar shield and the sequence of anomalous torques. The radiation pressure associated with this illumination, even combined with Earth's infrared (IR) blackbody radiation, would have been far too weak to torque the spacecraft noticeably. This line of reasoning seemed to be another dead end.

The recorded torques could have been produced, however, if the IR radiation were heating and sublimating ejecta from the spacecraft that had frozen to the back of the solar shield. As the other candidate theories, which at first seemed more likely, were disproved, the freezing and then boiling of outgassed matter was analyzed more carefully.

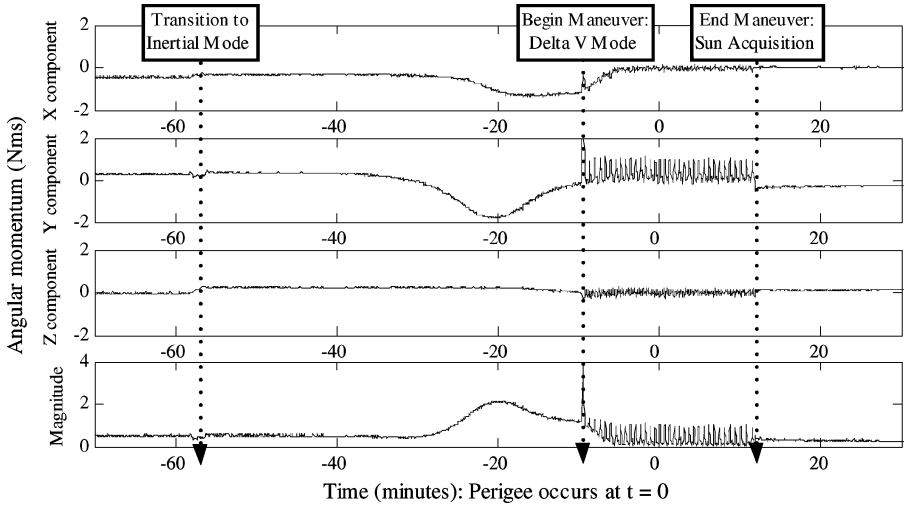

Fig. 4 System angular momentum profile at the first perigee maneuver.

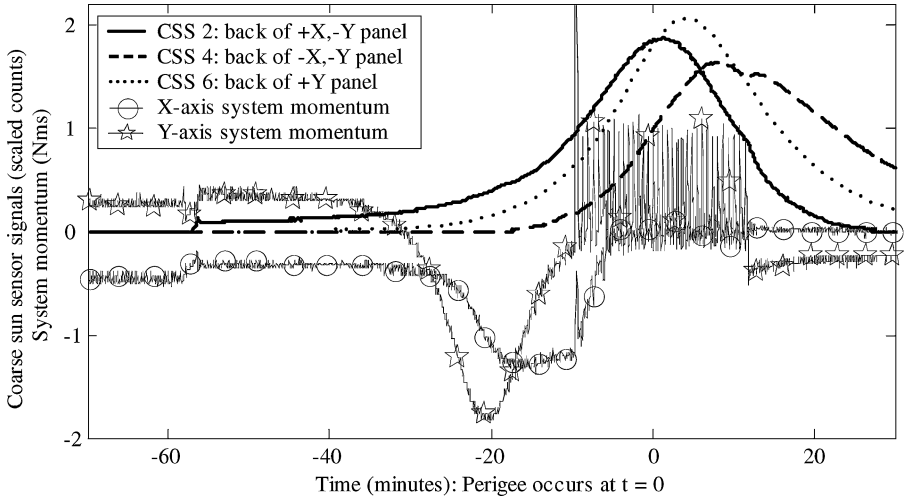

Fig. 5 First perigee: system momentum and coarse sun sensor responses to Earth albedo.

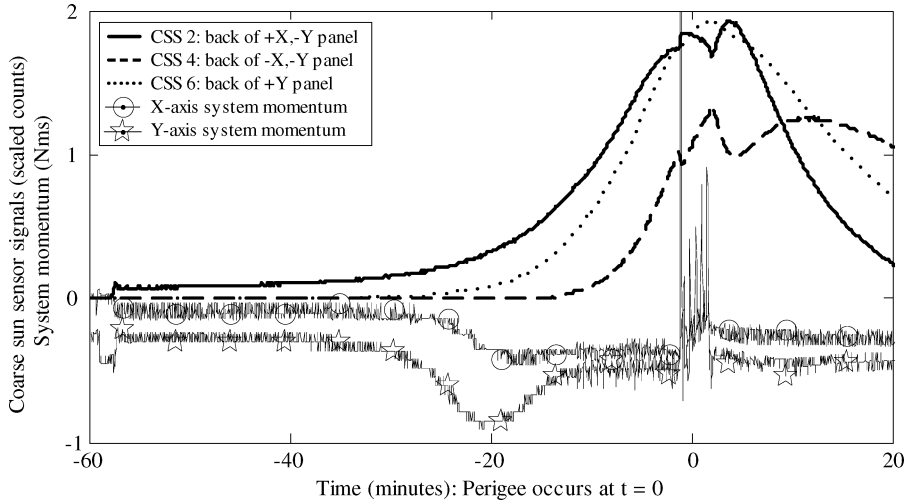

Fig. 6 Second perigee: system momentum and CSS responses to Earth albedo.

Outgassing

As mentioned before, the attitude profile leading up to the perigee maneuvers was unique in that the cold surfaces of the instrument and the solar shield were illuminated. It occurred to some team members that the instrument could be outgassing: first from the sunlit side and then from the other side as the instrument was heated by the sun. However, this outgassing would have produced first a positive pitching moment and then a negative moment, which was the opposite of the torque profile observed.

Soon after, it was noticed that the back of the solar arrays could see a similarly variable heating profile and that this heating profile could produce the correct torque profile. This theory was developed more thoroughly as the team gained more evidence to support it; the full development of the theory will be discussed in a later section. Meanwhile, in the absence of a predictive theory adjustments were made to the maneuver operations plan to be able to respond to further anomalies.

Operational Considerations

Because it was not known whether the anomalous behavior could recur or possibly worsen at subsequent perigee passes, preparations were made for the disabling of telemetry and statistics monitors (TSM) dealing with system momentum and the possible manual aborting of the next burn. Because the peak system momentum change decreased at each subsequent periapse, these special preparations had no effect on the P_2 or P_{final} maneuvers.

There were two concerns raised by the presence of this unanticipated force as the spacecraft approached perigee. First was a concern that the spacecraft attitude control might not perform within acceptable limits in the presence of the force. Second, because of the critical nature of the perigee-pass Delta V maneuvers there was a concern that the effects of the anomalous force would cause the spacecraft FDC logic to autonomously abort the burn. At best, a burn delay would have resulted in a large, additional expenditure of fuel. At worst, because of the precise timing demanded by the lunar swing-by there might not have been enough fuel to reach L_2, and so the mission could have been terminated.

Attitude Control System Performance

From the onset of the anomalous force and its resultant torque on the spacecraft, the attitude control system (ACS) was able to remove the disturbance with no obvious effect on pointing performance. This is because the anomalous force created a disturbance torque on the spacecraft of only 0.004 Nm, much less than the 0.215-Nm torque authority of each reaction wheel. So, the anomalous force would not have affected the ACS performance directly, but it could have affected performance indirectly through the system momentum buildup in the reaction wheels.

For the wheel-based control modes, system momentum buildup from the anomalous force was not likely to pose an ACS performance problem. Most of the various control modes could accommodate much higher momentum levels than those caused by the anomalies. However, the WMAP perigee environment had high

charged-particle densities that increased the risk of temporary outage of ACS hardware. The most basic safehold mode for WMAP is based on CSS measurements, and this mode was rated for a maximum momentum of 10 Nm · s.

In the two thruster-based control modes, performance concerns were more about initial transients into the mode than how well the control mode would perform at steady state because both Delta V and Delta H modes were effective in reducing system momentum. Any initial system momentum added by the anomalous force and still present at the beginning of the maneuver would have been removed by the action of the thruster mode during the maneuver. However, if the higher initial system momentum had caused the entry transient into Delta V mode to be unacceptably high onboard FDC would have aborted the burn.

FDC Configuration Changes

For the critical perigee-pass maneuvers, the FDC logic on the spacecraft, as implemented with ACS FDC points, TSMs, and relative time sequences (RTS) of commands, was put into its critical-burn configuration. This configuration used the bare minimum of TSMs and RTSs to keep the spacecraft safe in the event of a failure. Consideration of the entire FDC configuration revealed that the greatest danger from the anomalous force was that it could cause even the minimal safe FDC configuration to abort the burn.

Leading up to and during the P_1 orbital maneuver, there were three TSMs enabled that might have aborted a maneuver caused by system momentum buildup. The first two, the yellow and red high-system-momentum TSMs, were designed to detect system momentum buildup itself. The yellow high-system-momentum TSM was designed to detect a system momentum magnitude over 5 Nm · s. If tripped, the TSM would execute an RTS that would abort a maneuver and put the spacecraft into sun acquisition mode. The red high-system-momentum TSM was similar, except that this TSM looked for a higher system-momentum magnitude of 13 Nm · s, and it would also close the propulsion system isolation valves. In addition to these two TSMs, there was a Delta V performance TSM that would abort a burn if the attitude or rate error in the burn were too high; such an error could have been caused by a momentum-induced transient response.

As the system momentum magnitude increased during the first encounter with the anomalous force, the yellow high-system-momentum and Delta V performance TSMs were of primary concern. If the system-momentum magnitude had reached 5 Nm · s, the maneuver would have aborted. Even though that limit was not reached, the initial transient might still have been worse than actually occurred and could have tripped the Delta V performance TSM. When the momentum peaked at approximately 2.5 Nm · s, it was expected that the maneuver would perform nominally.

Operations at Second Perigee Pass

As P_2 approached, several reasonable theories for the cause of the anomalous force had been discredited, but no certain answer was yet forthcoming. Therefore, preparations were made to ensure that if the anomaly recurred with greater force FDC would not needlessly abort the P_2 or P_{final} maneuver.

During the time between the P_1 and P_2 maneuvers, simulations were run on FlatSat, the high-fidelity dynamic simulator for WMAP, to examine the effects of momentum buildup on the initial attitude and rate error transient into Delta V mode. The simulations indicated that the system-momentum buildup would not cause an increased transient performance error, and so the Delta V performance TSM was not a problem. Therefore, if the anomalous force caused a greater system momentum buildup than at P_1 the greatest risk of aborting a maneuver was still through the yellow high-system-momentum TSM. The following strategy was adopted to mitigate this risk.

As part of the sequence of commands used to implement the perigee maneuver, additional commands were included. The yellow high-system-momentum TSM was disabled before the expected onset time of the anomalous force for two reasons: 1) to allow a greater level of system momentum buildup prior to the maneuver and 2) to survive any unexpected initial transient into Delta V mode and allow Delta V to decrease system momentum. The red high-system-momentum TSM was still left in place to provide safety for the spacecraft. Five seconds after the maneuver began, after the initial transient into Delta V mode, the yellow high-system-momentum TSM was autonomously reenabled.

In addition to the preceding TSM changes, contingency procedures were prepared to perform a contingency momentum dump using thrusters in Delta H mode before the maneuver, if necessary. Also, plans were made to resume the maneuver quickly if prematurely aborted. The mission operations team closely monitored the system momentum prior to the maneuver to be ready to enact the contingencies in the event of a problem.

Development and Modeling of the Water Sublimation Theory

Collection of Frozen Material

After the maneuvers and subsequent sun acquisition, portions of the cold side of the Observatory rapidly cooled by radiating to space. Within about one day after exposure, by design, many surfaces on or with significant view to the WMAP instrument cooled below the temperatures at which outgassing byproducts could easily boil off in high vacuum. This condition caused materials that came into contact with these cold surfaces to have a significant capture probability. At the same time, the sunlit side of the solar shield was very warm and could continue to outgas, as could the blanketing for elements that produced their own heat.

As a result, the cold surfaces served as a cryogenic collector, or getter, for the outgassed material from the warm portions of the Observatory. It was observed that the solar shield fills approximately one-third of the spacecraft central truss field of view, allowing outgassed matter to be ejected and to freeze on the shield. In addition to spacecraft blanketing on the exterior hub, the blanket venting paths for the instrument and inner-hub liner blankets are directed at the cold side of the array panels through a pair of low-conductance vent apertures.

A review of the possible outgassing byproducts from the blankets indicated that the dominant component ought to be water. The humidity and temperature of sensitive components were monitored prior to launch to ensure the safety of the Observatory. Given the observed prelaunch environmental profile, the effective surface area of blankets, the on-orbit thermal profile, and the venting path and getter geometry, the best estimate of water mass available to settle on the back of the solar shield was in the range of 0.2–1.4 kg.

It was theorized that, once deposited, the ice needed to be warmed above about 130 K to have sufficient energy to boil off in high vacuum. Earth IR exposure was thought to be sufficient to sublimate the products on the back of the solar shield during maneuver operations. This premise is supported by thermal data recorded by the instrument package during the perigee maneuver. The key question was whether the temperature of the outer layers of the solar-array panel was cold enough to efficiently capture the outgassing products; the answer provided by the WMAP thermal subsystem team at the time was affirmative.

The order of magnitude of the average velocity[4] for the sublimating material, under the assumption that its dominant component was water, was estimated as

$$V_{\text{kin}} = \sqrt{2k_b T/uN} = 370\,\text{m/s} \tag{1}$$

$T \sim 150$ K, and $N = 18$ amu for H_2O. For the P_1 momentum anomaly, a peak magnitude of $H_{\max} \sim 2$ Nm · s was observed. Assuming $R = 1.5$ m, the anomalous force observed corresponded to an ejected mass of about

$$\Delta m = H_{\max}/2RV_{\text{kin}} = 0.002\,\text{kg} \tag{2}$$

Therefore, a collected-and-sublimated mass of about 0.002 kg of water could have produced the torques seen at P_1. This amount is small compared to the ~1-kg estimate for the total outgassing mass for the Observatory. Only a fraction of the total outgassing mass

could be expected to freeze to the cold solar shield, but Eqs. (1) and (2) do show that the effect is not excluded by our knowledge of the parameters of the system.

The data are essentially consistent with a uniform buildup of material. However, if the back of the solar-array blanket were uniformly heated the deposited material would only slightly perturb the angular momentum of the Observatory because torque response is a result of differential thrust experienced by spacecraft. The final piece of the puzzle was that the release of material on one portion of back of solar-array panel was delayed in time by the instrument and central hub shadowing some panels from Earth IR and albedo. This hypothesis was supported by telemetry from the CSSs on the cold side of the solar shield: CSSs 2, 4, and 6.

Relationship Between Attitude and Torque

The spacecraft Z axis was inclined roughly 45 deg with respect to the Earth nadir during its final approach to each maneuver, and the orbital velocity vector laid approximately between the $+X$ axis and the $+Z$ axis. CSS 2 was located on the leading edge of the spacecraft ($+X$ axis: see Fig. 2) and indicated when that edge was exposed to albedo, and approximately, to IR as well. However, CSSs 4 and 6 were not illuminated at the same time; rather, the midpoint CSS 6, on the $-Y$ axis, was lit second, and the CSS 4, on the trailing edge of the shield, was lit third. Figures 5 and 6 show how the time histories of the illumination of cold-side CSSs coincided with the changes in torque direction.

Putting the pieces together provides a coherent story of what happened during each perigee passage. When the $+X$-axis side of the shield was lit, the water sublimated and imparted a force to that side, resulting in a negative (nose-up) pitching moment. Because of orbit geometry, the nadir vector had a small $-Y$ component in the body frame. The result was that more of the $+Y$ side of the shield was shaded for longer, there was less sublimation on that side, and the balance of force provided a negative rolling moment. The time that this force was felt coincided with the lighting of the midpoint cold-side CSS 6. Finally, just before the maneuver the nadir vector moved more into alignment with the $-Z$ axis (cold side), and the trailing side of the shield moved out of shadow and became exposed to Earth radiation. As the trailing side was lit, CSS 4 was illuminated, and the sublimation of frozen material created a positive pitching moment approximately equal to the earlier negative moment.

Predictive Modeling

To establish that the Earth and moon would be sufficient thermal sources to quickly heat the solar shield, they were modeled as gray bodies based upon reference parameters, e.g., albedo, temperature, radius,[5,6] and the distance from the source to the spacecraft. The reflective Kapton thermal blanketing on the WMAP has a ratio of absorptivity to emissivity of 0.7. For all four cases, these thermal factors were found to allow for the rapid heating of the cold side of the solar shield to temperatures that would release ice. This result was confirmed by the thermal telemetry, as just mentioned.

An inverse dependence of mass deposition with time, $\mathrm{d}m/m = -\mathrm{d}t/\tau$, was expected as the system relaxed by outgassing to its final state. Because each heating event was of a similar illumination geometry and thermal profile, it was reasonable to assume that the peak momentum buildup would be proportional to the integral of the mass deposited since the previous event. Recalling that the material was frozen as it came into contact with the blankets, we integrated probability to find the total amount of material available to provide torque at each heating encounter. The integral is given by Eq. (3):

$$m(n)/m_o = e^{-t(n+1)/\tau} - e^{-t(n)/\tau} \tag{3}$$

Table 2 compares the observed momentum buildup and the buildup predicted by this simple model. The time constant of $\tau \sim 9$ days was appropriate for the geometry and composition of the spacecraft for this portion of the anticipated outgassing profile and is consistent with data obtained in thermal vacuum testing and previous flight experience.

Figure 7 shows the same comparison as Table 2, but scaled by the total amount of water that the model indicates was available for outgassing. (Figure 8 shows the momentum vs time histories before each perigee.) Thus, an observed momentum disturbance is associated with a corresponding percentage of available water; for example, a scaled momentum of 0.7 in Fig. 7 represents the

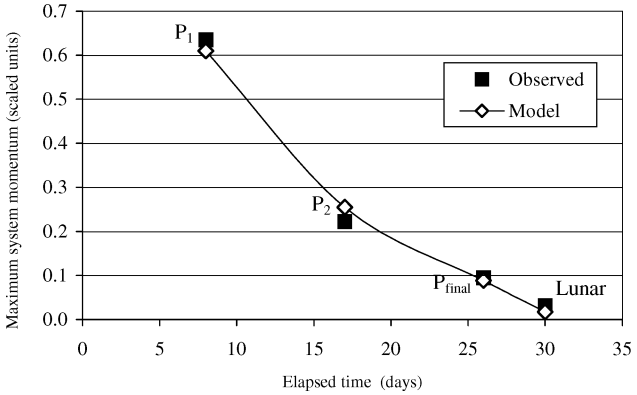

Fig. 7 Observed momentum compared to predictions of the water sublimation model.

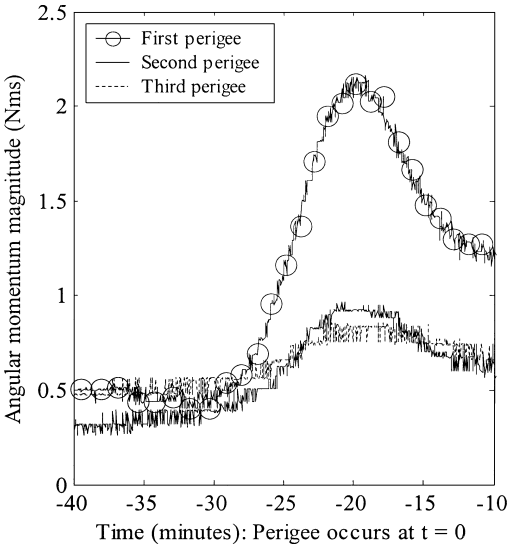

Fig. 8 Total angular momentum magnitudes just before the three perigee maneuvers.

Table 2 Observed torques vs torques predicted by the water capture-and-sublimation model

Event	Day of year	Outgassing time, days	Momentum magnitude, Nm · s	Observed torque,[a] %	Model torque,[a] %	Perigee altitude, km
Launch	181	0	——	——	——	——
P_1	189	8	2	100	100	3095
P_2	198	17	0.7	35	42	2952
P_{final}	207	26	0.3	15	14	4738
Periselene	211	30	0.1	5	3	5279

[a]Torques given as percentages of those observed at P_1.

disturbance caused by about 70% of the available water. According to the model, the sum for the four events yields that about 97% of the available water had outgassed before the periselene, leaving a maximum of about 3% of the water to affect the spacecraft at some later date. Because this figure is associated with the very small disturbance observed at periselene and because there would be no more maneuvers requiring the same finesse and timing as the perigee maneuvers, it was concluded that the outgassing and freezing of water represented no further threat to the mission.

Conclusions

Between the second and third perigee passes, a clear picture had emerged of how water outgassed from the thermal blanketing could cause the anomalies. The theory was applied to knowledge of the spacecraft design and prelaunch environment to develop a simple predictive model. That model indicated that the force would no longer present a threat to the spacecraft; still, the team was ready to respond in case the model was in error. At P_{final}, the observed momentum levels corresponded well with the model (see Fig. 8 for a comparison of the three perigee events). In addition, the model accurately predicted the occurrence of some small changes in system momentum at periselene—an occurrence no one had otherwise foreseen.

By design, the thermal control coatings on the passively cooled portions of the structure radiatively cool much faster than the outgassing timescales. For the WMAP mission, the time interval between accumulation and subsequent reheating and ejection of the outgassing products was compatible with the overall attitude control capability. The maneuvers were, in the end, untroubled by the anomalies, and WMAP is currently operating nominally in orbit near L_2.

The development of a more sophisticated collection and heating model, with an accurate depiction of the distribution of frozen material, might have been useful in proving that the torques seen were indeed caused by sublimating material. However, even the most detailed model would have had to include some significant assumptions nonetheless. For example, one major assumption needed to determine a distribution of vented material would have been the extent to which the venting flap had opened after launch. The strength of the simple model described here was that by comparing the magnitudes of the events the exact conditions did not need to be used to generate torque values. Instead, the knowledge of the P_1 and P_2 events was used to advantage in preparing for the most critical maneuver at P_{final}. In the end, the model's prediction of the unexpected momentum change at periselene was taken as satisfactory evidence to accept the hypothesis.

Important lessons can be gained from this flight experience. Given actual constraints on ability to control the prelaunch environment for the spacecraft, the effect just discussed should be considered in mission design and planning for a cooled system. If ignored, systems with large, passively cooled surfaces and significant potential for outgassing could experience a loss of torque storage or software design margins. In the design phase, this effect can be mitigated by limiting the view of cryogenic surfaces to likely outgassing vent paths and exploration of mission profiles that allow the system to bake out in flight prior to the passive cooling phase. Alternatively, mission designers could build in periodic dumping by means of IR exposure to limit the buildup of frozen material.

References

[1]Bennett, C. L., Hinshaw, G. F., and Page, L., "A Cosmic Cartographer," *Scientific American*, Vol. 284, No. 1, 2001, pp. 44, 45.

[2]Markley, F. L., Andrews, S. F., O.Donnell, J. R., and Ward, D. K., "The Microwave Anisotropy Probe (MAP) Mission," AIAA Paper 2002-4578, Aug. 2002.

[3]Larson, W. J., and Wertz, J. R. (eds.), *Space Mission Analysis and Design*, Microcosm, Inc., Torrance, CA, 1991, p. 353.

[4]Reif, F., *Fundamentals of Statistical and Thermal Physics*, McGraw–Hill, New York, 1965, pp. 265–273.

[5]Lang, K. R., *Astrophysical Formulae*, 2nd ed., Springer-Verlag, New York, 1980, p. 526.

[6]Allen, C. W., *Astrophysical Quantities*, 3rd ed., Athlone Press, London, 1976, pp. 139–152.

C. A. Kluever
Associate Editor